# A high-rate long-range wireless transmission system for multichannel neural recording applications

Henrique Miranda, Vikash Gilja, Cindy Chestek, Krishna V. Shenoy and Teresa H. Meng
Stanford University, Stanford, CA 94305
Email: {hmiranda, gilja, cindyc, shenoy, thm}@stanford.edu

***Abstract*—We report a high-rate, low-power wireless transmission system (named HermesD) to aid the research in neural prosthetics for motor disabilities, by recording and transmitting neural activity from electrode arrays implanted in rhesus monkeys. This system supports the simultaneous transmission of 32 channels of broadband data sampled at 30 kSps, 12 bit/sample, using FSK modulation on a 3.95 GHz carrier, with a link range extending over 20 m. The channel rate is 24 Mbit/s and the bit stream includes synchronization and error detection mechanisms. The power consumption, approximately 142 mW, is low enough to allow the system to operate for about two days, using two 3.7 V / 1100 mAh Li-Ion battery packs. The transmitter was designed using off-the-shelf components and is small enough to fit on a printed circuit board with 20 cm². The receiver is composed of several submodules in a bench-top configuration and interfaced to a computer for data storage and processing. This system can be easily scaled up in terms of the number of channels and data rate, being an appropriate test platform for a future 96-channel version of the system.**

***Index Terms*—Neural prosthetics, *in vivo* neural recording, wireless high-rate multichannel biotelemetry, high-rate FSK transmitter**

## I. Introduction

Neural recordings from freely behaving animals is an emerging area of neuroscience research. The approach described here could enable the study of complex behaviors that are inaccessible in an experimental rig such as social behavior, locomotion, or navigation [1]. Using a wireless approach, algorithms can now be tested in a less constrained setting. For human clinical systems, neural implants with transcutaneous connections should ideally be avoided since they are a potential source of infections. Optimally, the wireless telemetry device would also be implanted along with electrode array and power source. Several groups are developing single chip systems that may eventually be small enough to enable a fully implantable solution. However, this often means that they are not optimized for neuroscience research. For example, several systems usually require the external use of a power coil [2] which cannot be worn by a freely moving animal. Similarly, they are often designed for short range wireless transmission [3]. Due to power and bandwidth limitations, single chip systems often compress data, transmitting lower resolution signals [2] or threshold crossings from individual action potentials [4]. In contrast, for neuroscience research, a large animal such as a monkey can carry a substantial power supply, which can be changed every 24 hours as part of an experimental routine. Also, both action potential waveforms, as well as lower frequency neural signals such as electrocorticograms and local field potential are relevant to these neurological studies. Given these different constraints, it was logical to design a system optimized for neuroscience research using inexpensive off-the-shelf hardware.

Several implementations of high-rate multi-channel wireless transmitters for neurological acquisition systems using off-the-shelf components have been reported earlier. Rizk [2] proposes a 96-channel, 1 Mbit/s system capable of transmitting only one channel of broadband data at a time using a 150 mW transmitter. Obeid [5] took a rather different approach that employed an embedded computer and WLAN equipment to implement a wearable telemetry system. It is capable of transmitting 12 channels of broadband neural data and requires 4 W of power, which is far too high for multi-day recordings. Other multi-channel analog based transmitter systems can be economical in terms of power consumption as no analog-to-digital conversion stage is required [3]. However, it is very difficult to control their signal fidelity under various channel impairments such as multipath or shadowing.

To meet the required specifications at sufficiently low power and small size for use with a *rhesus macaque*, we have developed HermesD, which provides 32 channels of neural data sampled at 30 kSps. It is mainly targeted for neuroscience research applications that involve multi-day freely behaving experiments. It also provides the unique capability to transmit neural data up to 20 m, allowing the study of macaques embedded in social colonies or outdoor settings.

## II. HermesD system

The HermesD transmitter is implemented using only COTS components and was designed to be housed in an aluminum enclosure secured to the primate's head, similar to the one described in [6].

The neurological signals are captured by a 400 μm pitch 10×10 micro-electrode array developed at the University of Utah [7]. HermesD was designed to process 32 of the 96 channels provided by the electrode array, with possible future expansion to support all the available channels.

Wireless transmission occurs at about 3.95 GHz and the system can be easily tuned to any frequency between 3.7 GHz and 4.1 GHz. There are a few reasons for the choice of this frequency range. First, the allocated services for the band, mainly commercial satellite broadcast, pose virtually no risk of interference to this system, and vice versa. Secondly, the frequency is high enough to enable the design of small high efficiency antennas like the one built for HermesD. Lastly, a high carrier frequency also enables the use of high bandwidth signals to accommodate high bit-rates — important for scalability purposes. During the experiments, monkey subjects are usually housed in cages with a small mesh aperture (in the order of 2.5×2.5 cm²). If low carrier frequencies are used (below 1 GHz), the cage attenuation can be very significant. We performed attenuation tests that showed little attenuation at 4 GHz.

The frequency shift keying (FSK) modulation method was choosen since it enables a low power modulator implementation and a simpler receiver design where non-coherent techniques can be employed.

The RF output power of the transmitter, approximately 100 μW, is enhanced by an antenna gain of 7 dB, providing enough power to cover a range over 20 m with a comfortable link margin of about 20 dB.

### A. Transmitter

The detailed HermesD transmitter block diagram is shown in Fig. 1 and its blocks are described next:

978-1-4244-3828-0/09/$25.00 ©2009 IEEE

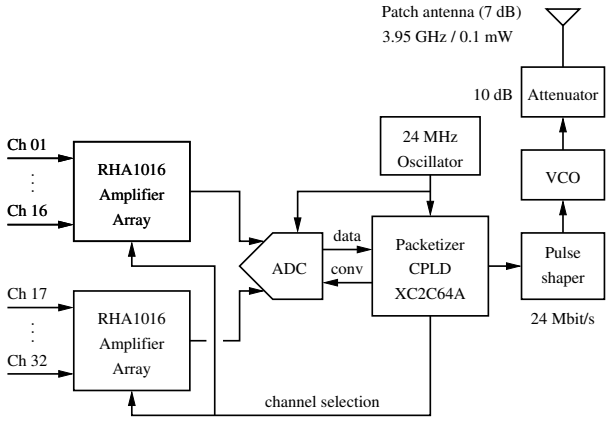


Fig. 1. HermesD transmitter block diagram

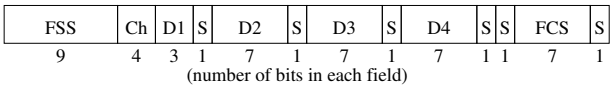


Fig. 2. HermesD frame format

*1) Ampli er array and ADC:* The 32 neural channels are amplified and filtered by two 16-channel biopotential array amplifiers from Intan Tech, LLC (RHA1016) [8]. These provide 46 dB of voltage gain, a configurable upper cut-off frequency ranging from 10 Hz to 10 kHz (set to 5 kHz in our experiments), and a lower cut-off frequency fixed at 0.05 Hz. Channels are multiplexed before being digitized by the dual channel analog-to-digital converter (ADC), the Linear Technology LTC1407A-1. Both multiplexed outputs from the amplifier arrays are sampled simultaneously and converted into 12-bit samples. The value of each LSB was set to 1.5 μV, slighlty less than the input referred noise of the amplifiers (2 μVrms), and spike amplitudes can be as high as 6.3 mV before clipping occurs.

*2) Stream packetizer and frame structure:* The stream packetizer collects samples from the ADC and organizes them in structured frames that contain additional information for synchronization and error detection. The packetizer is implemented in a Xilinx XC2C64A 64-macrocell CPLD (Complex Programable Logic Device), with an utilization ratio of about 65%. The CPLD was successfully tested up to 58 MHz (clock frequency), a limit considerably higher than the value used by HermesD at 24 MHz. As this frequency also sets a limit on the bit rate, this same CPLD configuration can be used for future HermesD versions with a higher channel count, as discussed in section IV. The frames, whose format is depicted in Fig. 2, contain 50 bits and are transmitted back-to-back. The frame fields and their purpose are the following: Frame Sync Sequence (FSS), a 9-bit synchronization pattern of alternating zeros and ones (010101010) that indicates the start of the frame; Channel (Ch), a 4-bit channel number being scanned by the amplifier arrays; Data fields (D1 – D4), a pair of 12-bit samples from the selected channels; and the Frame Check Sequence (FCS), a 7-bit checksum that is used to validate data integrity. The frames also contain stuffing bits (S fields) that are added at the end of every group of 7 bits, starting after the FSS. These bits are simply the repetition of the previous bit value, thus avoiding the FSS pattern to appear inside the frame and causing frame synchronization misalignments. The sampling frequency per channel is determined by $f_{\mathrm{clk}}$, the system clock frequency, and $N$, the number of bits in the frame, using $f_{\mathrm{s}} = f_{\mathrm{clk}}/(16N) = (24\times10^{6})/(16\times50) = 30$ kSps.

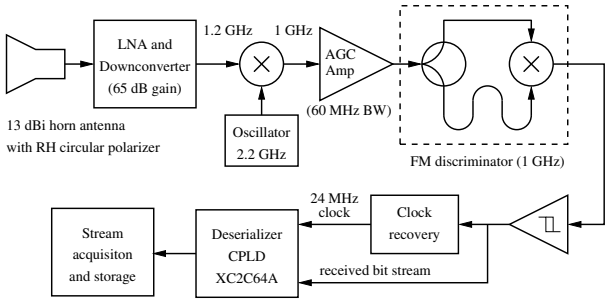


Fig. 3. HermesD receiver block diagram

*3) Modulator:* The FSK modulator is built around a miniature VCO module, the SMV3895A from Z-Communications, Inc. The output frequency is set by a simple resistor divider and the VCO is left in free running mode. No frequency stabilizing mechanism is used, such as a PLL, due to power saving reasons. In fact, as the occupied bandwidth of the modulated signal is fairly large (approximately 60 MHz), the VCO frequency stability is not a major concern. The typical temperature drift of this VCO is about 0.5 MHz/°C, which for a temperature controlled room like the one where the experiments take place, is low enough to have any impact on the system. To further enhance the frequency stability, a 10 dB attenuator was inserted at the output of the VCO so that the frequency pulling effect is mitigated. This effect is caused by the impedance variation of the antenna in its occasional proximity to external objects.

This VCO has a low modulation input capacitance ($C_{\mathrm{in}} \approx 11$ pF), making it suitable for wide signal bandwidths. In HermesD, the source impedance driving the VCO is $R_{\mathrm{s}} = 100\ \Omega$, setting the maximum modulation bandwidth to $\mathrm{BW}_{\mathrm{mod}} = 1/(2\pi R_{\mathrm{s}} C_{\mathrm{in}}) = 145$ MHz allowing a much higher data rate than currently used (24 Mbit/s).

The frequency deviation for the FSK signal was adjusted to a maximum of ± 20 MHz and was limited by the available receiver bandwidth (60 MHz).

*4) Antennas:* The transmitter antenna sits on top of the aluminum housing and is based on a microstrip patch design, which allows a very low profile construction: the patch area is 24×24 mm² and the substrate used is 3.2 mm thick made out of Teflon (RO5880 from Rogers Corp.). The antenna has an impedance bandwidth of 420 MHz centered at 3.95 GHz. The measured gain was 7.0 dB and is efficiency efficiency is 88%. The antenna can cover a full hemisphere with a maximum signal variation of 15 dB, which is well within the system signal margin for a 20 m link distance. This wide spatial antenna coverage is a desirable feature for reliable communications when the animal subjects are freely moving.

Both receiver and transmitter antennas employ circular polarization. This is particularly useful to attenuate first order reflections (single bounce) that occur in an indoor environment, which are the main cause for signal fluctuation due to destructive interference. All odd order reflections have their polarization rotation sense reversed, which are attenuated by the receiving antenna configured for the transmitter polarization.

### *B. Receiver*

The HermesD receiver (Fig. 3) is mostly built from readily available RF modules and is based on the classical superheterodyne architecture. Its main blocks are discussed as follows:

*1) RF and IF sections:* The received signal is captured by a 13 dBi conical horn antenna coupled to a waveguide circular polarizer compatible with the transmitted polarization type.

In the first receiver stage there is a low-noise downconverter block (LNB) that amplifies (65 dB of gain) and downshifts the incoming

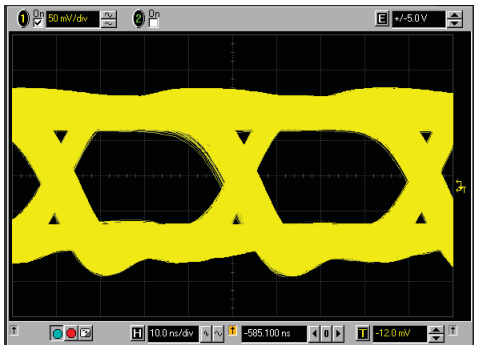

Fig. 4. Received signal eye diagram at 3 m of separation

frequency to 1.2 GHz. There is a second intermediate frequency conversion stage that serves two purposes: 1) receiver tunability by varying the oscillator frequency; 2) frequency shift to the band center of the automatic gain control amplifier (1 GHz). This amplifier provides a constant output level to the demodulator for 70 dB of input signal power variation and can process signal bandwidths up to 60 MHz.

*2) FM discriminator:* A custom FM demodulator was implemented and it is based on the delay line architecture shown inside the dashed block of Fig. 3. The discriminator mixer produces a voltage that varies as the $cos(\Delta\phi)$, $\Delta\phi$ being the phase difference between the input ports of this mixer. This phase difference is generated by using different lengths for the transmission lines connecting the signal splitter to this mixer. The demodulator main design parameter is the transmission line length difference ($\Delta l$) and the following procedure is used to obtain its value:

1) from the required frequency deviation ($f_d$) and center frequency ($f_c$), the integer number of odd multiples of 90° phase shifts in the extra $\Delta l$ length, k, is determined using $k = (f_c/f_d + 1)/2$ ;
2) then, $\Delta l$ is found from the velocity of propagation in the transmission lines ($v_p$) using $\Delta l = (2k-1)(v_p/f_c)/4$;

The $\Delta l$ parameter also directly influences the maximum transition rate that the demodulator can sustain while keeping the same maximum amplitude deflection at its output. Given the demodulator nature, the maximum theoretical rate (also the FSK bit rate) is limited to $R_{\max} = v_p/\Delta l = 4f_c/(2k-1) = 4f_d$, which corresponds to a modulation index $h = 2f_d/R$ of 0.5. Due to the band limiting nature of other components in the system and to make the clock recovery circuit more tolerant to jitter, $2fd$ is a more practical limit for $R_{\max}$ ($h = 1$).

In the specific case of HermesD, the following parameters are used: $f_c = 1$ GHz, $f_d = 25$ MHz, $v_p = 2 \times 10^8$ m/s (RG-174 coaxial cable); $k = 20$; $\Delta l = 1.95$ m; and $h = 2.1$. With these parameters a usable $R_{\max}$ of 50 Mbit/s is possible. Note that $f_d$ is set to 5 MHz larger than the frequency deviation used for the HermesD signal in order to accommodate carrier frequency offsets A snapshot of the demodulated signal eye diagram at 24 Mbit/s with a transmitter-receiver separation of 3 m on a bench-top setup is displayed in Fig. 4. The eye diagram is sufficiently open for an error free operation under correct bit sampling instants.

*3) Bit synchronizer:* Bit synchronization is achieved by the clock recovery circuit, which is based on a single transistor oscillator with injection locking (synchronous oscillator) [9]. It has several attractive features that are exploited in this system: its acquisition time is very fast, less than 1 µs, corresponding to less than half a frame, and thus keeps a low number of lost frames during aquisition; wide tracking range — 1% of the clock frequency — which is wide enough for the transmitter bit clock frequency tolerance (±100 ppm); and the circuit complexity is very low and easy to tune by varying just one capacitor value.

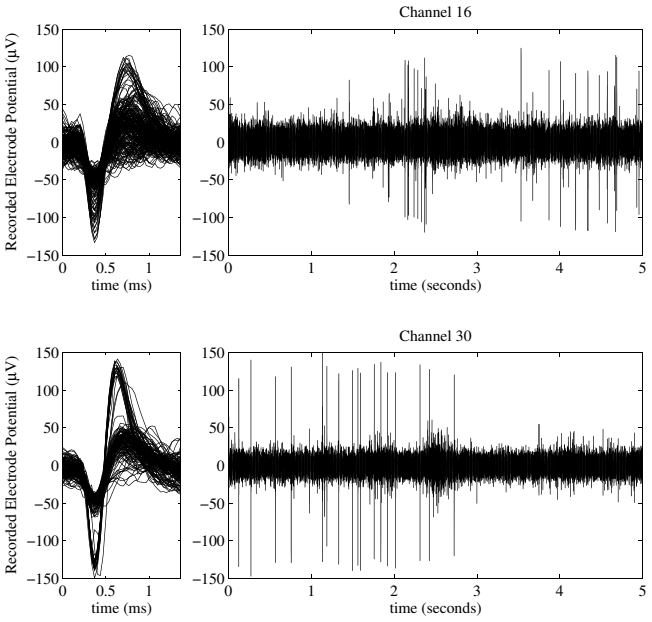


Fig. 5. Wireless *in vivo* recording of spontaneous neural activity of a *rhesus monkey* (signal for electrodes 16 and 30).

*4) Computer interface:* The receiver also includes a CPLD to convert the recovered serial data stream into a 32-bit parallel bus for computer storage. This bus has a clock rate 32 times lower than the incoming serial stream (750 kwords/s) which makes the computer data acquisition more efficient and cost effective. The digital I/O interface device is a National Instruments USB-6259. Frame storage, synchronization, disassembly and error check are performed off-line by software developed in the C and Matlab languages.

## III. Results

This system was used to obtain neural data *in vivo*. One adult male *rhesus macaque* was implanted with a 96-electrode array (I2S, Salt Lake City, UT [7]) using standard neurosurgical techniques similar to those described in [10] 8 months prior to the current study. All of the surgical procedures were approved by Stanford University's Institutional Animal Care and Use Committee (IACUC.) The HermesD prototype was tested inside a neuroscience rig while the animal was seated in a primate chair. A wired adapter was used to attach the device to the neural connector less than 20 cm from the implant. All 32 channels of neural data were received wirelessly at a distance of 1 m in this recording experiment.

### A. Neural data recordings

Some of the initial recordings performed are shown in Fig. 5. Samples acquired by the receiver were aligned sequentially in time based upon when the corresponding frame was recovered. In order to produce the two panels on the right, a second order high-pass butterworth filter with a 250 Hz cutoff frequency was applied to the data. The root mean squared (RMS) error was estimated from 150 seconds of recorded data by taking the standard deviation of the channel. Note that this assumes a negligible contribution from neural spikes. For the channels shown, from top to bottom, the RMS values measured were 11.9 µV and 11.7 µV. In order to find neural spikes in the data, a threshold of three times the RMS value was set. If this

TABLE I
POWER BREAKDOWN OF HERMESD

| **Device** | Amp. Array | ADC | CPLD | VCO | OSC | **Total** |
|---|---|---|---|---|---|---|
| **Power (mW)** | 68 | 14 | 26 | 30 | 5 | **142** |

value was crossed, a snippet of data around this time was extracted and a shape heuristic was applied. This heuristic filters for events in which the negative deflection is followed by a positive deflection. Action potentials recovered from 20 seconds of broadband data from the two plotted channels are shown on the left panels. Note that multiple distinct neural units are present on each of these channels.

## IV. POWER AND SYSTEM SCALABILITY

Power consumption in wireless implants is the major parameter to be optimized since one desires long recording times with the smallest battery volume possible. The largest power contributor for the HermesD transmitter is its analog section as shown in Table I. The power supply subsystem includes three switching regulators (5.0, 3.0 and 1.8 V) whose overall efficiency is 87%, adding an additional 21 mW of dissipation. Power is provided by two parallel-connected 3.7 V Li-Ion battery packs with a capacity of 1100 mAh each, the same batteries used in [6].

The HermesD architecture was designed with scalability in mind. Increasing the number of simultaneous transmitted channels is just a matter of adding more amplifier arrays and ADCs. No other hardware modifications are required since the CPLD and modulator can currently handle higher data rates (in excess of 50 Mbit/s). On the receiver side, the AGC and demodulator bandwidths are the only parameters that need to be matched to the new data rates. For the 96-channel scenario, a 52 Mbit/s data rate would be required using 108 bit frames. The estimated power consumption would be 340 mW and 60% of this power would be dissipated by the amplifier arrays while the VCO and oscillator consumptions would remain essentially the same.

## V. DISCUSSION

HermesD is able to wirelessly transmit, receive and store 32 channels of broadband neural data at a rate of 30 kSps with a resolution of 12 bit/sample, from a freely behaving primate. The power consumption of the system is sufficiently low to make it possible to operate for about two days from two small and lightweight batteries before recharge. This time period is long enough for many different experiments to be conducted with freely behaving animals.

### A. Future developments

The recordings performed with HermesD show good signal quality and absence of noticeable interference from the switching activity of the digital section of the transmitter circuit. A very small fraction of the frames were reported with errors, at a rate of less than 0.1%. This corresponds to an average loss rate of 30 samples/s/channel, which is, nonetheless, a very tolerable data loss since we can easily apply interpolation to "recover" those lost samples. It was experimentally verified that the synchronizer was loosing track for a very small fraction of time, caused by occasional long runs of ones or zeros in the frames. This could be avoided by using self-synchronizing line codes that prevent these bit events from occurring, such as the Coded Mark Inversion or Manchester codes. Increasing the receiver bandwidth, which is currently limited to 60 MHz, will enable not only the use of these line codes but also the increase of the number of channels. A higher receiver bandwidth version is currently being planned.

### B. Applications

Recently, there has been increased interest in using several kinds of neural signals for neural prosthetics. For example, it may be possible to combine spike waveforms with lower frequency local field potential, or record simultaneously from electrocortical arrays as well as high-impedance electrode arrays. HermesD allows these types of signals to be recorded simultaneously in experiments with freely moving animals. Beyond neural prosthetic applications, the long range of this system enables experiments with animals in a far less constrained environment. Several labs do behavioral research on rhesus macaques embedded in social colonies. With this device, it would be possible to record neural activity from an animal interacting freely with other animals in a complex setting. This represents a fundamentally new source of data for the neuroscience community that may lead to important new discoveries about the processing algorithms of the cerebral cortex.

## ACKNOWLEDGMENT

We thank Mackenzie Risch for expert surgical assistance and veterinary care, Stephen Ryu for expert neurosurgical leadership, Drew Haven for technical consultation, Rachel Kalmar and Zuley Rivera for animal training and care, Reid Harrison for technical consultation and donation of the Intan Inc. amplifier array chips, and Sandy Eisensee for administrative support. We also thank Rogers Corp. for donating the antenna microwave substrate. This study was supported by the NSF Graduate Research Fellowships (C.A.C., V.G.), William R Hewlett Stanford Graduate Fellowship (C.A.C.), NDSEG Fellowship (V.G.), Fundação para a Ciência e Tecnologia fellowship (H.C.M), The McKnight Endowment Fund for Neuroscience (K.S., T.H.M.) and the following awards to K.V.S.: The Christopher and Dana Reeve Foundation, Stanford Center for Integrated Systems. The authors acknowledge the support of the Focus Center for Circuit & System Solutions (C2S2), one of five research centers funded under the Focus Center Research Program, a Semiconductor Research Corporation Program.

## REFERENCES

[1] U. Jurgens and S. Hage, "Telemetric recordings of neuronal activity," *Methods*, vol. 38, pp. 195–201, 2006.

[2] M. Rizk, I. Obeid, S. Callender, and P. Wolf, "A single-chip signal processing and telemetry engine for an implantable 96-channel neural data acquisition system," *J. Neural Eng.*, vol. 4, no. 3, pp. 309–321, Sep. 2007.

[3] P. Mohseni, K. Najafi, S. Eliades, and X. Wang, "Wireless Multichannel Biopotential Recording using an Integrated FM Telemetry Circuit," *IEEE Trans. Neural Syst. Rehabil. Eng.*, vol. 13, no. 3, pp. 263–271, Sep 2005.

[4] C. Chestek, V. Gilja, P. Nuyujukian, S. Ryu, K. Shenoy, R. Kier, F. Solzbacher, and R. Harrison, "HermesC: RF Wireless Low-Power Neural Recording System for Freely Behaving Primates," in *IEEE ISCAS*, May 2008, pp. 1752–1755.

[5] I. Obeid, M. Nicolelis, and P. Wolf, "A Multichannel telemetry system for single unit neural recordings," *Journal of Neuroscience Methods*, no. 133, pp. 33–38, 2003.

[6] G. Santhanam, M. Linderman, V. Gilja, A. Afshar, S. Ryu, T. Meng, and K. Shenoy, "HermesB: A continuous Neural Recording System for Freely Behaving Primates," *IEEE Trans. Biomed. Eng.*, vol. 54, no. 11, pp. 2037–2050, Nov 2007.

[7] E. Maynard, C. Nordhausen, and R. Normann, "The Utah intracortical electrode array: a recording structure for potential brain-computer interfaces," *Electroencephalography and Clinical Neurophysiology*, vol. 102, no. 3, pp. 228–239, Mar. 1997.

[8] Intan Technologies, LLC, *Fully Integrated 16-Channel Biopotential Ampli er Array*, Salt Lake City, UT, Sep 2006, http://www.intantech.com/products.html.

[9] V. Uzunoglu and M. White, "The synchronous oscillator: A synchcronization and tracking network," *IEEE J. of Solid-State Electronics*, vol. SC-20, no. 6, pp. 1214–1226, Dec 1985.

[10] N. Hatsopoulos, J. Joshi, and J. O'Leary, "Decoding continous and discrete behaviors using motor and premotor cortical ensembles," *J. Neurophysiol.*, vol. 92, pp. 1165–1174, 2004.